

Conformations and Interactions of Star-Branched Polyelectrolytes

A. Jusufi, C.N. Likos,* and H. Löwen

Institut für Theoretische Physik II, Heinrich-Heine-Universität Düsseldorf, Universitätsstraße 1, D-40225 Düsseldorf, Germany

(Received 27 July 2001; published 14 December 2001)

Combining monomer-resolved molecular dynamics simulations with a theory based on a variational free energy, we calculate the conformational properties and the effective interactions of star-branched polyelectrolytes for a large variety of arm numbers, degrees of polymerization, and charge fractions, with and without added salt. We find quantitative agreement between theory and simulation and put forward analytical expressions that allow the calculation of the interaction between such macromolecules.

DOI: 10.1103/PhysRevLett.88.018301

PACS numbers: 82.70.-y, 61.20.-p, 82.35.Rs

Polyelectrolytes (PEs) are polymer chains containing ionizable groups. Upon solution into a polar solvent, these groups dissociate, leaving behind a system of charged chains and counterions. The study of PEs has been the subject of many recent investigations [1–7]. When these charged chains are grafted on solid surfaces, they form PE brushes; when their ends are brought together to a common point, they form PE stars. Conformations and interactions of planar PE brushes have also been studied in some detail, using scaling theory, self-consistent field (SCF) calculations, and computer simulations [8–11]. Spherical PE brushes and stars are much less well understood. These are systems of great physical and practical importance: grafting of PE chains on colloidal particles greatly enhances their stability against flocculation [12,13]; PE brushes are models of block copolymer micelles formed by hydrophobically modified PEs in aqueous solutions [14], and they have considerable potential in industrial applications due to the increased need for water-supported systems [15]. PE stars interact by means of three physical mechanisms: the electrostatic interaction of their charges, the steric repulsion between the chains, and the entropic repulsion of their counterions. The pioneering work on star-shaped PEs goes back to Pincus [12], who predicted that the force between two PE stars should be dominated by the entropic contribution of the counterions. Recently, Borisov *et al.* put forward a scaling theory, together with SCF calculations to study the conformations of isolated PE stars [14,16]. However, a systematic investigation of the *interactions* of the same, by means of computer simulations and an analytical theory valid for *both* isolated and interacting PE stars, is still lacking. In the present work, we employ molecular dynamics (MD) simulations and a variational theory to study the sizes, conformations, and interactions of PE stars for high charging fractions. We find a stretching of the chains and significant counterion condensation and we confirm Pincus' prediction [12] explicitly.

In our MD simulations, we have f chains with N monomers per chain, all attached on a common microscopic core. The chains are charged periodically: every $1/\alpha$ bead carries an elementary charge $|e|$, yielding $Q = \alpha f N$ charges in the star and Q oppositely charged

counterions. The simulation model was introduced by Stevens and Kremer [17] for linear PE chains. The monomers are modeled as spherical beads interacting by means of a truncated and shifted Lennard-Jones potential [18], with energy $\varepsilon_{LJ} = k_B T / 1.2$ and length scale σ . A finite-extendible-nonlinear-elastic (FENE) potential [19] binds the adjacent monomers along the chains and the Coulomb interaction acts between all charged units. The solvent has dielectric constant ϵ ; the Bjerrum length is $\lambda_B \equiv e^2 / (\epsilon k_B T)$. We take $\lambda_B = 3.0\sigma$, a realistic value for typical hydrophilic polyelectrolytes [20] ($\sigma \cong 2.5 \text{ \AA}$) in water ($\lambda_B = 7.14 \text{ \AA}$). The Lekner method [21] is employed for the Coulomb sums. We considered PE stars with $f = 5, 10, 30,$ and 50 arms, with $N = 50$ monomers, and $\alpha = 1/6, 1/4,$ and $1/3$.

We first consider a single PE star in a cubic simulation box with an edge length of $L = 90\sigma$, which defines the density $\rho_s = L^{-3}$ of the solution, and periodic boundary conditions. After a sufficiently long equilibration time, different static quantities were calculated: radii of gyration R_g , center-to-end distances R , correlation functions of the bond vectors of the beads, as well as density profiles of all species involved. Moreover, we measured the average number of counterions N_{in} inside the radius R of the star and the fraction thereof that was condensed along the rods, by surrounding every charged monomer with a fictitious sphere of radius λ_B and monitoring the number of counterions inside all spheres. A scaling behavior of the profile as a function of the distance from the star center was found, with a slope ~ -1.8 , pointing to a stretched chain configuration. The fully rodlike limit of the PE chains yields a slope value of -2 [14,16] and has been seen in neutron scattering studies of block copolymer micelles [22]. Because of lateral chain fluctuations [2–5,23], the measured slope is somewhat smaller, it indicates nevertheless an almost complete stretching of the chains. The counterion profile showed the same r dependence as the monomer one, due to the tendency of the system to achieve local charge neutrality.

In the theory, we consider a star in a dilute solution of density ρ_s and define accordingly the Wigner-Seitz radius $R_W = (4\pi\rho_s/3)^{-1/3}$. Following Ref. [14], we envision

the star as a sphere of radius R enclosed in a cell of radius $R_W > R$; all counterions are restricted to move inside the cell R_W . Particular attention has to be paid to the Manning condensation of counterions on the chains [1–7,24–26], which takes place when the parameter $\xi = \lambda_B N \alpha / R$ exceeds unity [24]. This condition is satisfied for all our parameter combinations, as summarized in Table I. Hence, we partition the Q counterions into three states and write $Q = N_1 + N_2 + N_3$. N_1 is the number of condensed counterions on the rods of the star, N_2 are those who are trapped inside the star but move freely there, and N_3 stay in the region $R < r < R_W$. Since we are in the regime where the ratio λ_B / σ is of order unity, the condensed counterions can move freely along the rod direction [4]. Accordingly, we introduce tubes of length R and radius λ_B surrounding each rod and treat all counterions contained in these tubes as condensed. The interior volume $V(R) = 4\pi R^3 / 3$ of the star is divided as $V(R) = V_1 + V_2$ with $V_1 = f\pi(\lambda_B^2 - \sigma^2)R$ being the total volume of the hollow tubes available to the condensed counterions, and V_2 the volume available to the N_2 mobile counterions inside. Moreover, let $V_3 = 4\pi(R_W^3 - R^3) / 3$ be the volume of the spherical shell for the free counterions, and $\rho_i(r)$, $i = 1, 2, 3$, the number densities of the three counterion states.

The equilibrium values for R and N_i are determined through minimization of the variational free energy

$$\mathcal{F}(R, \{N_i\}) = U_H + U_c + F_{\text{el}} + F_{\text{Fl}} + \sum_{i=1}^3 S_i, \quad (1)$$

where the various terms have the following meaning: $U_H = (1/2\epsilon) \int \int d^3r d^3r' \varrho(\mathbf{r})\varrho(\mathbf{r}') / |\mathbf{r} - \mathbf{r}'|$ is the Hartree-type, mean-field electrostatic energy of the whole star with the local charge density $\varrho(\mathbf{r})$ to be defined below. We assume that the only relevant correlations arise between the condensed counterions and the charges

TABLE I. Comparison of conformational properties between simulation and theory. The polymerization of the chains is $N = 50$ for all entries. The last two rows show the same properties for N_s added salt counterions, and they correspond to salt concentrations $c_s = 0.088M$ and $c_s = 0.109M$, respectively.

f	α	Q	R/σ^a	R/σ^b	N_{in}^a	N_{in}^b	N_1^a	N_1^b
5	1/3	80	26.8	26.1	47	57	27	25
10	1/6	80	23.4	23.7	42	59	22	38
10	1/4	120	25.3	25.2	77	97	46	61
10	1/3	160	27.4	26.9	110	134	72	81
18	1/6	144	24.2	25.8	91	121	60	90
18	1/4	216	26.6	26.9	156	190	107	141
18	1/3	288	28.3	28.1	217	260	159	190
f	α	N_s	R/σ^a	R/σ^b	N_{in}^a	N_{in}^b	N_1^a	N_1^b
10	1/3	600	22.6	22.7	156	155	54	71
10	1/3	750	21.8	22.1	164	156	56	74

^aSimulation.

^bTheory.

on the chains. Hence, the correlation energy U_c stems from the attractions between the rods and the condensed counterions contained in the associated tubes. We estimate the average rod-condensed counterion separation as $z_m = (1/2)\sqrt{\lambda_B^2 + y_m^2}$, where $y_m = R/(N\alpha)$ is the distance between two sequential charged monomers along the chain, obtaining $U_c = -k_B T \lambda_B N_1 / z_m$. The term $F_{\text{el}} = 3k_B T f R^2 / (2N)$ is the elastic contribution of the chains and the term $F_{\text{Fl}} = 3k_B T \nu (fN)^2 / (8\pi R^3)$ the Flory-type contribution from the self-avoidance of the same, with the excluded volume parameter ν . Finally, the terms S_i are ideal entropic contributions of the form $S_i = k_B T \int_{V_i} d^3r \rho_i(r) \ln \rho_i(r)$.

The chains are modeled as being fully stretched; i.e., the density distributions inside the stars fall off as $\sim r^{-2}$ from the center but are uniform outside the star. This is different from the approach of Ref. [14], where *uniform* densities inside and outside the star were employed. Reasonable results for the isolated star are obtained using uniform profiles; however, the nonuniform ones are of paramount importance for obtaining agreement with simulation results regarding the effective interaction. Accordingly,

$$\frac{\varrho(\mathbf{r})}{|e|Q_*} = \frac{\Theta(R-r)}{4\pi R r^2} - \frac{\Theta(r-R)\Theta(R_W-r)}{V_3}, \quad (2)$$

with the net charge $|e|Q_* = |e|(Q - N_1 - N_2)$ and the Heaviside step function $\Theta(x)$. The number densities are $\rho_1(r) = N_1/V_1$ inside the tubes and zero otherwise; $\rho_2(r) \propto r^{-2}\Theta(R-r)$, with the proportionality constant being determined through the condition $\int_{V_2} d^3r \rho_2(r) = N_2$; and $\rho_3(r) = \Theta(r-R)\Theta(R_W-r)N_3/V_3$. The value of the excluded volume parameter ν for stiff PEs has been the topic of extensive discussion [9,12,25]. Here, the estimate of Ref. [14], $\nu \cong \lambda_B \kappa^{-2} \alpha^2$, is used, with the inverse Debye length $\kappa = \sqrt{3N_2 \lambda_B / R^3}$. Taking typical values $N_2 \cong 40$, $R \cong 30\sigma$, $\alpha \cong 1/3$, we obtain $\nu \cong 25\sigma^3$. We subsequently employed the value $\nu = 30\sigma^3$; the theoretical results showed however a very weak variation with ν for values $20 \leq \nu/\sigma^3 \leq 40$ that we considered.

The results are summarized in Table I. The radii values from theory and simulation are in good agreement for all parameter combinations considered. Regarding the total number of trapped counterions $N_{\text{in}} = N_1 + N_2$ and N_1 of condensed counterions, we can make the following remarks: both are overestimated in the theory, by an amount depending on the charging fraction α . This overestimation can be explained by the fact that we assumed a complete stretching of the chains (rodlike configuration), which results in a stronger electrostatic attraction than the true one, in which lateral chain fluctuations are present. The same mechanism is responsible for the overestimation of N_1 . This claim is corroborated by the remark that the largest discrepancies occur for the smallest charge fraction, $\alpha = 1/6$, where the assumption of stretched chains is most questionable. On the other hand, the *ratio* of

condensed to absorbed counterions appears to be almost constant, $\sim 70\%$ for $f \gtrsim 10$, both in theory and simulation. The theoretical results have been obtained with a minimal amount of fitting: in particular, the value of the excluded volume parameter v has been held constant, despite its (weak) (f, N, α) dependence. However, a variation of v would obscure the clarity of the theory which, with the present, minimal assumptions, captures the salient features of the star conformations: it reproduces the tendency of the PE stars to increase the fraction N_{in}/Q of absorbed counterions as f and/or α increase, in line with the predictions of scaling theory in the “osmotic star” regime [16]. The theory can also be extended to the case of added salt by the addition of entropic terms for the counterions and coions. We have performed simulations for the salted case as well, finding, in full agreement with theory, that the addition of salt results in an almost complete neutralization of the PE star with increasing salt concentration c_s , to a shrinking of its radius and to an exclusion of all coions from the star interior; see Table I.

Next we consider the effective interaction $V_{\text{eff}}(D)$ between two PE stars kept at center-to-center distance D . $V_{\text{eff}}(D)$ results after taking a canonical trace over all but the star-centers degrees of freedom and is defined as $\mathcal{F}_2(D) - \mathcal{F}_2(\infty)$, where $\mathcal{F}_2(z)$ is the Helmholtz free energy of two PE stars at center-to-center separation z [27]. In a standard simulation, the effective force $\mathbf{F}(D) = -\vec{\nabla}V_{\text{eff}}(D)$ is measured [18,27]. By placing the star centers along the body diagonal of the cubic simulation box, we measured the effective force $\mathbf{F}(D)$ for various (f, N, α) combinations and for distances ranging from deep interpenetrations to barely nonoverlapping stars. We have checked that the image charges have only a minor effect in the measured forces at bare overlaps. In addition, we have carried out simulations in the presence of salt, which screens out the effects of image charges, finding similar agreement with theory as the one we report below for the salt-free case. We will report on the results for added salt in a future paper.

When two PE stars overlap, the chains of each star retract, a feature already conjectured by Pincus [12] and also confirmed in all our simulations. Hence, the two stars are modeled as “fused spheres,” each carrying the cloud of its untrapped counterions around it, as shown in Fig. 1. The chains remain otherwise stretched; hence a $\sim r^{-2}$ falloff of the density profile from each star center remains. Because of the retraction of the chains, the two profiles from each center do *not* overlap. Rather, each profile is sharply cut off as soon as the distance from the corresponding center reaches the bisecting plane located at a distance $D/2$ from the centers. The variational free energy $\mathcal{F}(D)$ is written as in Eq. (1).

For convenience, we separate the total charge density $\varrho(\mathbf{r})$ into two terms, $\varrho_{\text{in}}(\mathbf{r})$ in the interior of the fused spheres (V_{in}) and $\varrho_{\text{out}}(\mathbf{r})$ in the eight-shaped region outside (V_{out}). $\varrho_{\text{out}}(\mathbf{r})$ is homogeneous and equal to

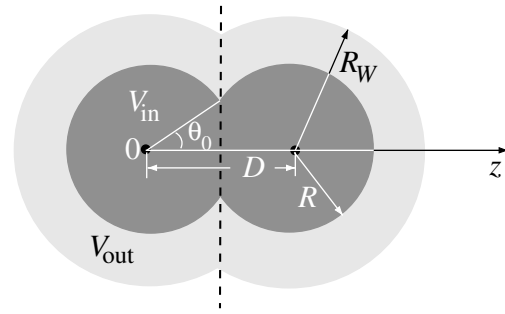


FIG. 1. Sketch of two PE stars at separation D .

$-|e|Q_*/V_{\text{out}}$. We choose a spherical polar coordinate system with its origin the center of the left star (see Fig. 1). Setting $r_\theta = r \cos\theta$ and $\omega \equiv \theta - \theta_0$, we write $\varrho_{\text{in}}(\mathbf{r}) = A|e|[P(\mathbf{r}) + P(\mathbf{D} - \mathbf{r})]$ with the shape function:

$$P(\mathbf{r}) = \frac{1}{r^2} [\Theta(R - r)\Theta(\omega) + \Theta(D/2 - r_\theta)\Theta(-\omega)], \quad (3)$$

where $A = Q_* \{4\pi R [1 + \cos\theta_0(1 - \ln \cos\theta_0)]\}^{-1}$ guarantees that $\int_{V_{\text{in}}} d^3r \varrho_{\text{in}}(\mathbf{r}) = |e|Q_*$. The term U_c remains unaffected by D and the elastic energy F_{el} is the sum of the two star contributions. The Flory free energy is $F_{\text{Fl}} = k_B T v (2fN)^2 / (2V_{\text{in}})$. The entropic terms S_i include now the D -dependent volumes of integration and corresponding profiles $\rho_i(\mathbf{r})$. In particular, $\rho_1(\mathbf{r})$ is uniform within the $2f$ tubes and zero otherwise. The trapped counterion density $\rho_2(\mathbf{r})$ has the form $\rho_2(\mathbf{r}) = B[P(\mathbf{r}) + P(\mathbf{D} - \mathbf{r})]$; see Eq. (3). The constant B is determined by the condition $\int_{V_2} d^3r \rho_2(\mathbf{r}) = N_2$, where $V_2(D) = V_{\text{in}}(D) - V_1$. Finally, $\rho_3(\mathbf{r}) = N_3/V_{\text{out}}(D)$.

The radius R is independent of D and equal to the single-star value, as a result of chain stretching. Moreover, the number of condensed counterions N_1 of both PE stars was treated in our considerations as a D -independent fit parameter, tuned in order to achieve optimal agreement with simulation, in analogy with the charge-renormalization technique used in the realm of charged colloidal suspensions [28,29]. If no charge rearrangement took place upon close approach, this value would be exactly twice the number of condensed counterions of a single PE star [30]. Our resulting values are within 15% of this number, pointing to the fact that the fit parameter is not arbitrary but rather it turns out to lie within physically acceptable limits.

The results for the force are shown in Fig. 2, showing good agreement between theory and simulation. The *shape* of the force is determined almost entirely by the entropic term S_2 and the electrostatic contribution U_H plays only a minor role, as the PE stars are almost electroneutral, in agreement with the predictions of Ref. [12]. A simple and accurate fit is given by $F(D) = CD^{-\gamma}$, with $0.7 \lesssim \gamma \lesssim 0.8$, and a constant $C > 0$. The precise γ value depends on α . The *magnitude* of the force is mainly determined by the amount of

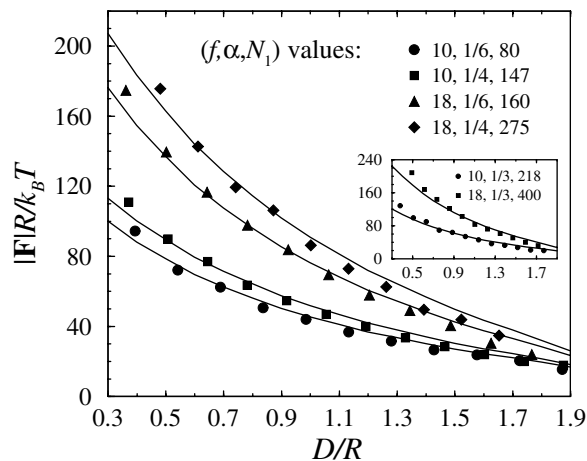


FIG. 2. Effective forces between two PE stars: comparison between theory (lines) and simulation (points). The inset axes have the same labels as those of the main plot.

mobile counterions $N_2 = N_{\text{in}} - N_1$ inside. The number of condensed counterions has in practice the effect of setting the scale of the force, in full analogy with the role played by the renormalized charge in charge-stabilized colloidal suspensions [29]. The force is considerably larger than the one acting between *neutral* stars ($\alpha = 0$) of the same N and f [18] and grows with increasing α , pointing to a charge-induced enhancement of colloid stabilization [12].

For the interaction beyond overlap, our theoretical calculations show that this has a Yukawa form. Matching of the two expressions for $D \leq 2R$ and $D > 2R$ leads then to the full interaction potential. The latter displays similar qualitative features as the interaction potential between neutral stars [31], i.e., a crossover from a Yukawa-like tail for large separations into an ultrasoft form for strong overlaps. Thus, we anticipate that the phase diagram of PE stars will show similar qualitative features as that of the neutral stars [32], namely, reentrant melting and a lower critical freezing arm number f_c below which the solution will remain fluid at all concentrations. In view of the fact that the present interaction is much stronger at overlap than the one for neutral stars, f_c will be smaller than the corresponding value 34 obtained for the latter [32]. Associated are anomalous structure factors displaying two independent length scales [32] and a principal peak whose height decreases beyond the overlap concentration. Hence, our effective interaction could be employed in understanding scattering profiles from concentrated PE star solutions [13,15,33].

We thank E. Allahyarov, M. Ballauff, and E. Rebhan for helpful discussions. This work has been supported by the Deutsche Forschungsgemeinschaft, Project No. LO418/7-1.

*Corresponding author.

Email address: likos@thphy.uni-duesseldorf.de

- [1] A. Yethiraj and C.-Y. Shew, Phys. Rev. Lett. **77**, 3937 (1996).
- [2] A. Yethiraj, Phys. Rev. Lett. **78**, 3789 (1997).
- [3] H. Schiessel and P. Pincus, Macromolecules **31**, 7953 (1998).
- [4] R. G. Winkler *et al.*, Phys. Rev. Lett. **80**, 3731 (1998).
- [5] N. V. Brilliantov *et al.*, Phys. Rev. Lett. **81**, 1433 (1998).
- [6] R. M. Nyquist *et al.*, Macromolecules **32**, 3481 (1999).
- [7] L. Harnau and P. Reineker, J. Chem. Phys. **112**, 437 (2000).
- [8] F. Vongoller and M. Muthukumar, Macromolecules **28**, 6608 (1995).
- [9] R. Hariharan *et al.*, Macromolecules **31**, 7506 (1998).
- [10] E. B. Zhulina *et al.*, Macromolecules **33**, 4945 (2000).
- [11] F. S. Csajka and C. Seidel, Macromolecules **33**, 2728 (2000).
- [12] P. Pincus, Macromolecules **24**, 2912 (1991).
- [13] X. Guo and M. Ballauff, Langmuir **16**, 8719 (2000).
- [14] J. Klein Wolterink *et al.*, Macromolecules **32**, 2365 (1999).
- [15] W. Groenenwegen *et al.*, Macromolecules **33**, 3283 (2000).
- [16] O. V. Borisov and E. B. Zhulina, J. Phys. II (France) **7**, 449 (1997); Eur. Phys. J. B **4**, 205 (1998).
- [17] M. J. Stevens and K. Kremer, J. Chem. Phys. **103**, 1669 (1995).
- [18] A. Jusufi *et al.*, Macromolecules **32**, 4470 (1999).
- [19] G. S. Grest, Macromolecules **27**, 3493 (1994).
- [20] For example, poly(acrylamide-co-sodium-2-acrylamido-2-methylpropane-sulfonate); see W. Essafi *et al.*, J. Phys. II (France) **5**, 1269 (1995).
- [21] J. Lekner, Physica (Amsterdam) **176A**, 524 (1991).
- [22] P. Guenoun *et al.*, Phys. Rev. Lett. **81**, 3872 (1998).
- [23] Y. Kantor and M. Kardar, Phys. Rev. Lett. **83**, 745 (1999).
- [24] G. S. Manning, J. Chem. Phys. **51**, 924 (1969).
- [25] T. Odijk and A. H. Houwaart, J. Polym. Sci. Polym. Phys. **16**, 627 (1978).
- [26] M. Deserno *et al.*, Macromolecules **33**, 199 (2000).
- [27] C. N. Likos, Phys. Rep. **348**, 267 (2001).
- [28] J.-P. Hansen and H. Löwen, Annu. Rev. Phys. Chem. **51**, 209 (2000).
- [29] N. Lutterbach *et al.*, Langmuir **15**, 345 (1999).
- [30] M. N. Tamashiro *et al.*, Physica (Amsterdam) **258A**, 341 (1998).
- [31] C. N. Likos *et al.*, Phys. Rev. Lett. **80**, 4450 (1998).
- [32] M. Watzlawek *et al.*, Phys. Rev. Lett. **82**, 5289 (1999); J. Phys. Condens. Matter **10**, 8189 (1998).
- [33] M. Heinrich *et al.*, Eur. Phys. J. E **4**, 131 (2001).